*Astronomy & Astrophysics* manuscript no. EBLM_J0555-57_production
July 13, 2017
©ESO 2017

arXiv:1706.08781v2 [astro-ph.SR] 12 Jul 2017

Letter to the Editor

# The EBLM project⋆

## III. A Saturn-size low-mass star at the hydrogen-burning limit

Alexander von Boetticher[1,2], Amaury H.M.J. Triaud[2], Didier Queloz[1,3], Sam Gill[4], Monika Lendl[5,6], Laetitia Delrez[1,9], David R. Anderson[4], Andrew Collier Cameron[7], Francesca Faedi[8], Michaël Gillon[9], Yilen Gómez Maqueo Chew[10], Leslie Hebb[11], Coel Hellier[4], Emmanuël Jehin[9], Pierre F.L. Maxted[4], David V. Martin[3], Francesco Pepe[3], Don Pollacco[8], Damien Ségransan[3], Barry Smalley[4], Stéphane Udry[3], and Richard West[8]

[1] Cavendish Laboratory, J J Thomson Avenue, Cambridge, CB3 0HE, UK
[2] Institute of Astronomy, Madingley Road, Cambridge CB3 0HA, UK
[3] Observatoire Astronomique de l'Université de Genève, Chemin des Maillettes 51, CH-1290 Sauverny, Switzerland
[4] Astrophysics Group, Keele University, Staffordshire, ST55BG, UK
[5] Space Research Institute, Austrian Academy of Sciences, Schmiedlstr. 6, 8042, Graz, Austria
[6] Max Planck Institute for Astronomy, Königstuhl 17, 69117 Heidelberg, Germany
[7] SUPA, School of Physics & Astronomy, University of St Andrews, North Haugh, KY16 9SS, St Andrews, Fife, Scotland, UK
[8] Department of Physics, University of Warwick, Coventry CV4 7AL, UK
[9] Université de Liège, Allée du 6 août 17, Sart Tilman, 4000, Liège 1, Belgium
[10] Instituto de Astronomía, Universidad Nacional Autónoma de México, Ciudad Universitaria, Ciudad de México, 04510, México
[11] Hobart and William Smith Colleges, Department of Physics, Geneva, NY 14456, USA

12. June, 2017

**ABSTRACT**

We report the discovery of an eclipsing binary system with mass-ratio q ∼ 0.07. After identifying a periodic photometric signal received by WASP, we obtained CORALIE spectroscopic radial velocities and follow-up light curves with the *Euler* and TRAPPIST telescopes. From a joint fit of these data we determine that EBLM J0555-57 consists of a sun-like primary star that is eclipsed by a low-mass companion, on a weakly eccentric 7.8-day orbit. Using a mass estimate for the primary star derived from stellar models, we determine a companion mass of $85 \pm 4 M_{\rm Jup}$ ($0.081 M_\odot$) and a radius of $0.84^{+0.14}_{-0.04} R_{\rm Jup}$ ($0.084 R_\odot$) that is comparable to that of Saturn. EBLM J0555-57Ab has a surface gravity $\log g_2 = 5.50^{+0.03}_{-0.13}$ and is one of the densest non-stellar-remnant objects currently known. These measurements are consistent with models of low-mass stars.

**Key words.** binaries: eclipsing; spectroscopic – Stars: low-mass – Stars: EBLM J0555-57Ab – techniques: spectroscopic; photometry

Eclipsing binary stars enable empirical measurements of the stellar mass-radius relation. The low-mass regime, down to the hydrogen-burning mass limit, is poorly constrained by measurements of mass and radius, but is of particular relevance to the study of exoplanets. Stars with masses below $0.25 M_\odot$ are the most common stellar objects (Kroupa 2001; Chabrier 2003; Henry et al. 2006) and prove to be excellent candidates for the detection of Earth-sized planets (Berta-Thompson et al. 2015; Gillon et al. 2016; Gillon et al. 2017; Luger et al. 2017) and their atmospheric characterization (de Wit et al. 2016). Determining the properties of exoplanets requires an accurate knowledge of their host star parameters, in particular the stellar mass. This motivates the study of low-mass eclipsing binaries (henceforth EBLMs) (Triaud et al. 2013; Gómez Maqueo Chew et al. 2014), to empirically measure the mass-radius relation. In this context, we report our results on the eclipsing binary EBLM J0555-57. The system was detected by the Wide Angle Search for Planets (WASP; wasp-planets.net; Pollacco et al. 2006), and was identified as a non-planetary false-positive through follow-up measurements with the CORALIE spectrograph. We use radial velocities and two eclipse observations by the TRAPPIST and *Euler* telescopes, to determine the mass and radius of EBLM J0555-57Ab, to $85.2^{+4.0}_{-3.0}$ $M_{\rm Jup}$ ($0.081 M_\odot$) and $0.84^{+0.14}_{-0.04}$ $R_{\rm Jup}$ ($0.084 R_\odot$). This places EBLM J0555-57Ab at the minimum of the stellar mass-radius relation.

## 1. Observations

The source 1SWASPJ055532.69-571726.0 (EBLM J0555-57, J0555-57 for brevity) was observed by WASP-South between 2008-09-29 and 2012-03-22. The *Hunter* algorithm (Collier Cameron et al. 2007) detected 17 transit-like signals from 34 091 observations over four seasons, at a period of 7.7576 days. We obtained 30 spectra of EBLM J0555-57A, using the high-resolution fibre-fed CORALIE échelle-spectrograph (Queloz et al. 2001), mounted on the *Euler* telescope, between 2013-11-14 and 2017-01-21.

Two eclipse observations in the near-infrared $z'$-band were obtained with the *Euler* (Lendl et al. 2013) and TRAPPIST (Gillon et al. 2011; Jehin et al. 2011) telescopes, on the nights of 2014-02-24 and 2015-12-23 respectively. The observations re-

*Send offprint requests to*: av478@cam.ac.uk
⋆ The data is publicly available at the CDS Strasbourg and on demand from the first author.

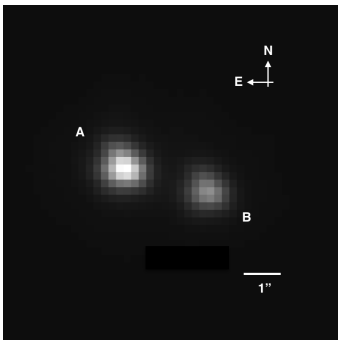


Fig. 1: Focused image (z'-band) of EBLM J0555-57 by *Euler*, resolving the eclipsed (A) and tertiary (B) components.

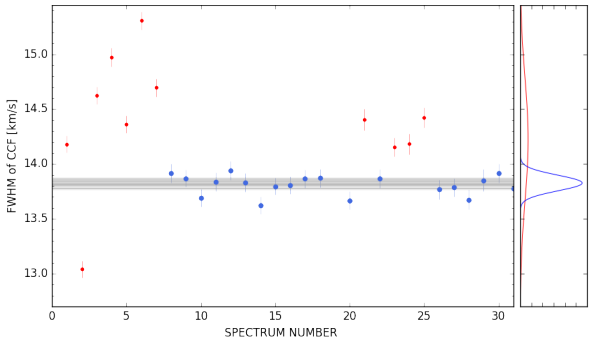


Fig. 2: FWHM of the CCF of the spectra of EBLM J0555-57A. Blue: clean sample, red: contaminated sample. Grey: random draws from the posterior of the clean sample.

veal that our target was blended by a star that we label as J0555-57B. To confirm the source of the transit signal we compared observations with a large 38-pixel (px) aperture encompassing both stars, and a small 16 px aperture centred on the brighter star. A deeper transit signal was observed with the small aperture, identifying J0555-57A as the source of the eclipse signal. One spectrum of EBLM J0555-57B was obtained. The systemic radial velocities of the A and B components, $\gamma_A = 19.537 \pm 0.015$ kms$^{-1}$ and $\gamma_B = 19.968 \pm 0.021$ kms$^{-1}$, are nearly identical. A very similar position angle of the B component is observed on (blended) 2MASS images from 1999 and the *Euler* image, which shows that A and B also share the same proper motion. This confirms that EBLM J0555-57A, B, and the transiting EBLM J0555-57Ab constitute a hierarchical triple system.

Focused images in the B, V, R, and $z'$-bands were obtained with *Euler* on 2014-02-23 and 2016-01-10. We measured the separation between the primary and blend star to be $2.48 \pm 0.01''$, with a position angle, PA $= -105.57 \pm 0.23°$. The magnitude difference, $\Delta z' = 0.753 \pm 0.035$ mag, translates into a flux-dilution of the eclipse depth by a factor $1.500 \pm 0.016$. The eclipse observations were reduced to obtain a photometric light-curve, as described in Lendl et al. (2012) and Delrez et al. (2014) for *Euler* and TRAPPIST, respectively. A significant out-of-transit observation before ingress was obtained, but few out-of-transit measurements after egress could be made. Using literature broadband optical photometry and 2MASS J, H, and K magnitudes for the A and B components combined, together with the multi-colour magnitude differences ($\Delta b = 0.95 \pm 0.01$ mag, $\Delta r = 0.786 \pm 0.017$ mag, $\Delta v = 0.832 \pm 0.014$ mag), we estimated IRFM temperatures (Blackwell & Shallis 1977) of $6450 \pm 200K$ and $5950 \pm 200K$ for the A and B components, respectively. A comparison to stellar model fluxes (Castelli & Kurucz 2004) was used, assuming a solar composition. The multi-colour observations and a *GAIA* DR1 parallax measurement (Gaia Collaboration et al. 2016) were used to derive individual radii, $R_A = 1.17 \pm 0.10 R_\odot$, and $R_B = 0.94 \pm 0.08 R_\odot$. The parallax and angular separation of the A and B components determine a projected outer semi-major axis $a_{AB,p} = 479 \pm 38$ au.

## 2. Data analysis

### 2.1. Radial velocities

Radial velocities of EBLM J0555-57A were extracted by cross-correlating individual spectra with a numerical G2 mask (Pepe et al. 2002). Varying seeing conditions resulted in fluctuations in the amount of flux from J0555-57B that enters the CORALIE fibre. This contamination can be identified by the full-width at half-maximum (FWHM) of the cross-correlation function (CCF). To select the non-contaminated spectra, we assumed two populations of points, a contaminated sample and a clean sample, with distinct means and variances. Following Hogg et al. (2010), a Markov chain Monte Carlo (MCMC) sampler was used to marginalise over the clean sample mean and variance, the contaminated sample mean and variance, and the prior probability that any point comes from the contaminated sample. We rejected a radial-velocity measurement and its associated spectrum when the FWHM had a posterior probability $< 1\%$ to originate from the clean distribution, as indicated in Fig. 2. We excluded one point with a discrepant value in the span of the bisector inverse slope.

### 2.2. Spectral Analysis

Atmospheric parameters were obtained via a wavelet-based Monte Carlo method (Gill et al. 2017). The 18 spectra identified as uncontaminated were median-combined onto an identically sampled wavelength grid. After continuum regions were determined and normalised with spline functions, the spectrum was decomposed using a discrete Daubechies ($k = 4$) wavelet transform. We filtered out wavelet coefficients that corresponded to high-order noise and low-order systematics, associated with poor continuum placement. A grid of models was generated with the radiative transfer code SPECTRUM (Gray & Corbally 1994), using MARCS model atmospheres (Gustafsson et al. 2008), and version 5 of the GES atomic line list using iSpec (Blanco-Cuaresma et al. 2016), with solar abundances from Asplund et al. (2009). Filtered coefficients were compared to those from the grid of models using an MCMC sampler implemented in emcee (Foreman-Mackey et al. 2013). We used four free parameters, $T_{\rm eff}$, [Fe/H], $\log g$, and $v \sin i_\star$, in the range 4000 – 8000 K (250 K steps), l3.5 – 5 dex (logg, 0.25 dex steps) and -1 – 1 dex (Fe/H, 0.5 dex steps).

The median value of the cumulative posterior probability distribution was used to estimate the atmospheric parameters for J0555-57A (Table 1). The precision associated with the wavelet method underestimates the uncertainty, so we adopt uncertainties by Blanco-Cuaresma et al. (2014) for the synthetic spectral fitting technique of *GAIA* FGK benchmark stars (124 K, 0.21 dex, and 0.14 dex for $T_{\rm eff}$, $\log g$, and [Fe/H], respectively). The spectroscopic temperature measurements, $T_{\rm effA} = 6461 \pm 124$ K (18 spectra) and $T_{\rm effB} = 5717 \pm 124$ K (1 spectrum) are consistent with the initial IRFM estimates.

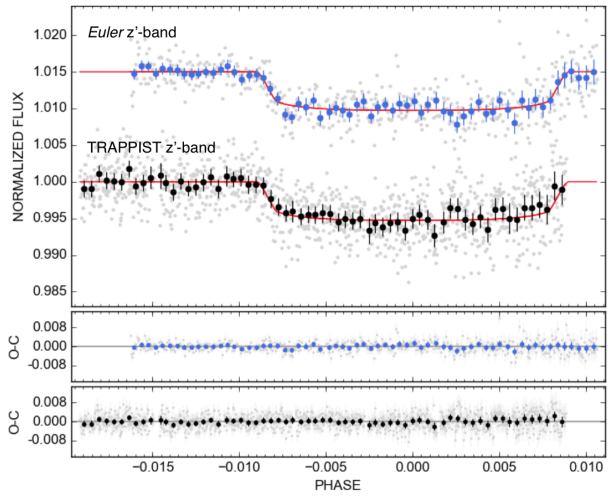


Fig. 3: Transits of EBLM J0555-57Ab, observed by *Euler* (top), and TRAPPIST (bottom), with the best-fit model and residuals shown in the lower panels.

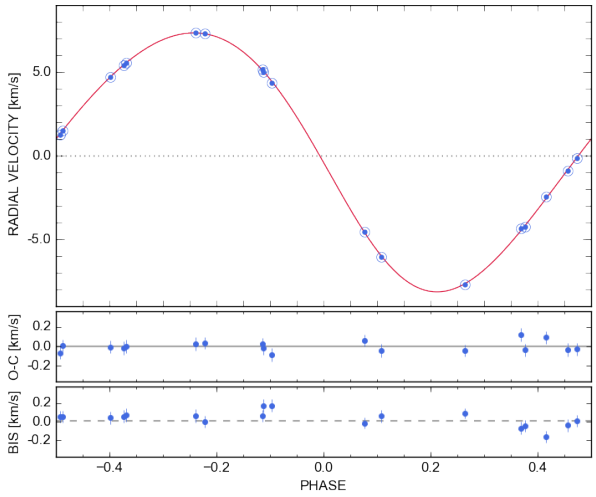


Fig. 4: CORALIE radial velocities and Keplerian model for EBLM J0555-57A. Uncertainties are smaller than the symbols. Lower panels: residuals and span of bisector inverse slope (BIS).

## 3. Model of the data

The radial velocity and light curves were modeled using the ELLC binary star model (Maxted 2016)[1]. An MCMC sampler (EMCEE; Foreman-Mackey et al. 2013), was used to fit the transit light-curves and radial velocities in a framework similar to that described in Triaud et al. (2013). We used the Bayesian information criterion (BIC) (Schwarz 1978) to compare detrending baselines of varying complexity in time-, position-, FWHM-, and background-dependence. A flat baseline with a linear background subtraction is preferred for both light curves. Indeed both observations show a large fluctuation in the background flux.

The parameters used in the MCMC sampling are the period $P$, the mid-transit time $t_0$, the observed transit depth $D_{\rm obs}$, the transit duration $W$, the impact parameter $b$, the semi-amplitude $K$, the parameters $\sqrt{e}\sin\omega$, $\sqrt{e}\cos\omega$, and the systemic velocity $\gamma$. The RV sample was separated into two parts, with distinct systemic velocities, to account for a change in the zero-point of CORALIE after a recent upgrade (Triaud et al. 2017). The geometric parameters of the system, $R_1/a$, $R_2/a$, and $i$ were derived from the MCMC parameters using the formalism from Winn (2010), and were then passed to ELLC. The TRAPPIST sequence was interrupted by a meridian flip; to account for a possible systematic offset in the flux measurement, an offset-factor was included for measurements before the flip.

We used a quadratic limb-darkening law in the MCMC analysis, with a Gaussian prior on coefficients that were interpolated from Claret (2004), using the spectroscopic parameters $T_{\rm eff}$, [Fe/H] and $\log g$. We included nuisance parameters in the MCMC sampler, that scale uncertainties in the photometry and radial velocity to account for white noise. The baseline parameters for a linear background subtraction, meridian flip, and normalization are fitted by a least-squares algorithm. Where not explicitly stated otherwise, we used unbounded, or sensibly bounded uniform priors to constrain parameters to physical intervals, for instance ($0 < e < 1$). The B-component dilutes the transit depth by a factor $f_d = f_{\rm A}/(f_{\rm A} + f_{\rm B})$, where $f_A$ and $f_B$ denote the flux from the A and B components respectively. We sampled a Gaussian prior on this depth dilution factor, $f_d = 1.500 \pm 0.016$, to compute the true transit depth $D_{\rm calc}$ at every step in the Markov chains. This calculated transit depth was used in the derivation of the physical parameters.

We analyzed this first global fit for correlated noise in the photometry (Gillon et al. 2012; Winn et al. 2008). The light curve was binned in the range of 10 to 30 min and the maximum root-mean square (RMS) deviation of the residuals in this bin range was determined. The flux uncertainties were then rescaled by the ratio of the maximum binned RMS deviation to the RMS deviation of the un-binned residuals. This increased the uncertainties by factors of 2.02 and 1.37 for TRAPPIST and *Euler* respectively. We then performed a global MCMC fit using 100 chains of 10 000 steps each.

The modes of the marginalised posterior distributions for each jump parameter are reported with upper and lower 68% confidence intervals. The physical parameters of the system were derived from the MCMC parameters, in particular the parameter $\log g_2$, which is independent of the primary star mass (Southworth et al. 2004). We used the primary star density to iteratively refine the primary mass estimate $M_1$. An initial primary density was estimated from the transit and was used to determine a primary mass using BAGEMASS (Maxted et al. 2014). BAGEMASS uses stellar evolution models by Weiss & Schlattl (2007). The primary star mass was then used with the transit and radial velocity model, to compute an updated density, and we proceeded iteratively. The calculated density was found to be consistent from the first iteration step.

## 4. Results

Independently of any assumptions for the primary star, we obtain a surface gravity $\log g_2 = 5.50^{+0.03}_{-0.13}$ for EBLM J0555-57Ab, comparable to that of the recently announced brown dwarf EPIC 201702477b (Bayliss et al. 2017). We determine a mass function f(m) = $0.0003686\,^{+0.0000037}_{-0.0000049}$ $M_\odot$. Using the primary star mass determined with BAGEMASS, we find a stellar companion with mass $85.2^{+4.0}_{-3.9}$ $M_{\rm Jup}$ ($0.0813^{+0.0038}_{-0.0037}$ $M_\odot$) and radius $0.84^{+0.14}_{-0.04}$ $R_{\rm Jup}$ ($0.084^{+0.014}_{-0.004}$ $R_\odot$). This implies a mass ratio $q = 0.0721^{+0.0019}_{-0.0017}$. A lower uncertainty in the radius measurement may be achievable by high-precision photometry (e.g. TESS; Sullivan et al. 2015). The fit of the radial velocity results in an RMS deviation of 65 $ms^{-1}$, and our analysis reveals a low but significant

[1] We validated ELLC on two EBLM systems published in Triaud et al. (2013), reaching a $1\sigma$-agreement on the derived parameters.

orbital eccentricity, $e = 0.0894^{+0.0035}_{-0.0036}$. The BIC of a forced circular fit, and the Lucy-Sweeney test (Lucy & Sweeney 1971) validate this orbital eccentricity, since its measurement is significant at ~25$\sigma$. The non-zero eccentricity of EBLM J0555-57Ab could indicate a previous orbital decay, for instance by Kozai-Lidov oscillations (Lidov 1961; Kozai 1962) induced by J0555-57B, or an undetected body, followed by tidal friction (Fabrycky & Tremaine 2007). At the current semi-major axis, a = 0.0817 au, such Kozai-Lidov oscillations are likely suppressed by general-relativistic precession (Fabrycky & Tremaine 2007; Petrovich 2014). It is unlikely that a contamination of the spectra causes the measured non-zero eccentricity, but further spectroscopic observations with a fibre of smaller diameter can clarify this. We note a discrepancy between the spectroscopic $\log g_{1\mathrm{spec}} = 4.18 \pm 0.21$ and that derived from the calculated radius and prior mass, $\log g_1 = 4.5^{+0.03}_{-0.13}$. Spectroscopic measurements of log$g$ are known to be poorly constrained (Torres et al. 2012; Bruntt et al. 2012; Doyle 2015). We verify that adopting a prior on $\log g_1$ for the spectroscopic analysis, using the derived value, leads to a primary and companion mass and radius that are consistent with the previous result.

We conclude that EBLM J0555-57Ab is located just above the hydrogen-burning mass limit that separates stellar and substellar objects (~ 83 $M_{\mathrm{Jup}}$ for objects with [M/H] = -0.5; Baraffe et al. (1998)). In Figure 5 we show the posterior distribution of J0555-57Ab on the mass-radius diagram for brown dwarfs and low-mass stars. Our results using BAGEMASS indicate an age of 1.9 ± 1.2 Gy for J0555-57A. The mass and radius of J0555-57Ab are consistent with models of a metal-poor, low-mass star. J0555-57Ab does not show evidence of a radius that is inflated, for instance by magnetic fields, as hypothesized by Lopez-Morales (2007) for low-mass stars. With its location on the lower bound of the mass-radius relation for stellar objects, J0555-57Ab is a critical object in the empirical calibration of the mass-radius relation in this regime. J0555-57Ab has a mass similar to that of TRAPPIST-1A. (Gillon et al. 2016; Gillon et al. 2017). The low radius of EBLM J0555-57Ab, comparable to that of the low-mass star 2MASS J0523-1403 (Dieterich et al. 2014), demonstrates the size dispersion for low-mass stars. It is essential that such variations are understood as we prepare for the detection of multi-planetary systems orbiting ultra-cool dwarfs by experiments such as SPECULOOS (Gillon et al. 2013).

*Acknowledgements.* We thank the anonymous referee for valuable comments that improved the manuscript. The Swiss *Euler* Telescope is funded by the Swiss National Science Foundation. TRAPPIST-South is a project funded by the Belgian Fonds (National) de la Recherche Scientifique (F.R.S.-FNRS) under grant FRFC 2.5.594.09.F, with the participation of the Swiss National Science Foundation (FNS/SNSF). WASP-South is hosted by the South African Astronomical Observatory and we are grateful for their ongoing support and assistance. L. Delrez acknowledges support from the Gruber Foundation Fellowship. M. Gillon and E. Jehin are Belgian F.R.S.-FNRS Research Associates. This work was partially supported by a grant from the Simons Foundation (PI Queloz, grant number 327127).

## References

Asplund, M., Grevesse, N., Sauval, A. J., & Scott, P. 2009, ARA&A, 47, 481
Baraffe, I., Chabrier, G., Allard, F., & Hauschildt, P. 1998, A&A
Baraffe, I., Homeier, D., Allard, F., & Chabrier, G. 2015, A&A, 577, A42
Bayliss, D., Hojjatpanah, S., Santerne, A., et al. 2017, AJ, 153, 15
Berta-Thompson, Z. K., Irwin, J., Charbonneau, D., et al. 2015, Nature
Blackwell, D. E. & Shallis, M. J. 1977, MNRAS, 180, 177
Blanco-Cuaresma, S., Nordlander, T., Heiter, U., et al. 2016, in 19th Cambridge Workshop on Cool Stars, Stellar Systems, and the Sun (CS19), 22
Blanco-Cuaresma, S., Soubiran, C., Heiter, U., & Jofré, P. 2014, A&A, 569, A111

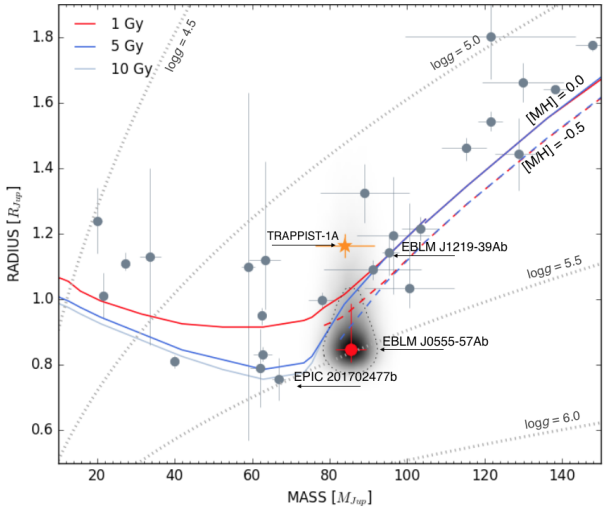


Fig. 5: Mass-radius posterior distribution for EBLM J0555-57Ab with an 68% confidence region (dashed). Isochrones for solar metalicity (Baraffe et al. 2015), and sub-solar metalicity [M/H = -0.5] (Baraffe et al. 1998) are plotted. Objects from Triaud et al. (2013); Ségransan et al. (2003); Demory et al. (2009); Bayliss et al. (2017); Díaz et al. (2014); Johnson et al. (2011); Siverd et al. (2012) and Chen et al. (2014) are also shown.

Table 1: Parameters of EBLM J0555-57A and Ab. The last two significant figures of the uncertainty are shown in brackets. Dates are $\mathrm{BJD_{UTC}}$ - 2 450 000. $R_{\mathrm{Jup}} = 69.911 \cdot 10^6$ km.

| 1SWASP J055532.69-571726.0<br>2MASS J05553262-5717261<br>TYC 8528-926-1; CD-57 1311 | | | |
|---|---|---|---|
| Parameter | | Parameter | |
| *Spectral line analysis of primary; system parameters* | | | |
| $T_{\mathrm{eff}}$ | 6461 ± 124 K | [Fe/H] | −0.24 ± 0.16 |
| $\log g_1$ | 4.18 ± 0.21 (cgs) | $v \sin i_1$ | 7.60 ± 0.28 km/s |
| d* | $193.8^{+14.5}_{-12.6}$ pc | Mag** | A: 9.98, B: 10.76 |
| *Parameters of MCMC* | | | |
| $P$ | $7.757676^{(+29)}_{(-25)}$ d | $t_0$ | $6\,712.6452^{(+15)}_{(-14)}$ |
| $D_{\mathrm{obs}}$ | $0.00474^{(+26)}_{(-21)}$ | $W$ | $0.1392^{(+49)}_{(-28)}$ d |
| $\sqrt{e}\cos\omega$ | $-0.176^{(+06)}_{(-06)}$ | $b$ | $0.35^{***}{}^{+0.24}_{-0.25}$ $R_\odot$ |
| $\sqrt{e}\sin\omega$ | $0.241^{(+09)}_{(-09)}$ | $K_1$ | $7.740^{(+27)}_{(-33)}$ km s$^{-1}$ |
| *Derived parameters from MCMC* | | | |
| $D_{\mathrm{calc}}$ | $0.00713^{(+41)}_{(-33)}$ | $f(m)$ | $0.0003686^{(+37)}_{(-49)}$ $M_\odot$ |
| $R_2/R_1$ | $0.0844^{(+23)}_{(-19)}$ | log $g_2$ | $5.50^{+0.03}_{-0.13}$ (cgs) |
| $R_1$/a | $0.0562^{(+88)}_{(-13)}$ | $R_2$/a | $0.00480^{(+79)}_{(-16)}$ |
| $M_1$ (prior) | 1.13 ± 0.08 $M_\odot$ | $M_2$ | $85.2^{+4.0}_{-3.9}$ $M_{\mathrm{Jup}}$ |
| $R_1$ | $0.99^{+0.15}_{-0.03}$ $R_\odot$ | $R_2$ | $0.84^{+0.14}_{-0.04}$ $R_{\mathrm{Jup}}$ |
| $\rho_1$ | $1.16^{+0.1}_{-0.42}$ $\rho_\odot$ | $\rho_2$ | $188^{+25}_{-69}$ g cm$^{-3}$ |
| $a$ | $0.0817^{(+19)}_{(-19)}$ au | $i$ | $89.84^{+0.2}_{-1.8}$ deg |
| $e$ | $0.0894^{(+35)}_{(-36)}$ | $\omega$ | $-53.7^{+1.5}_{-1.8}$ deg |
| $q$ | $0.0721^{(+19)}_{(-17)}$ | | |

**Notes.** (*) from GAIA parallax (**) GAIA g-magnitude (***) The mode is ambiguous so the median value is provided.

Bruntt, H., Basu, S., Smalley, B., et al. 2012, MNRAS, 423, 122
Castelli, F. & Kurucz, R. L. 2004, ArXiv e-prints, arXiv:astro-ph/0405087v1
Chabrier, G. 2003, PASP, 115, 763
Chen, Y., Girardi, L., Bressan, A., et al. 2014, MNRAS, 444, 2525
Claret, A. 2004, A&A, 428, 1001
Collier Cameron, A., Wilson, D. M., West, R. G., et al. 2007, MNRAS, 380, 1230
de Wit, J., Wakeford, H. R., Gillon, M., et al. 2016, Nature, 537, 69
Delrez, L., Van Grootel, V., Anderson, D. R., et al. 2014, A&A, 563, A143
Demory, B.-O., Ségransan, D., Forveille, T., et al. 2009, A&A, 505, 205
Díaz, R. F., Montagnier, G., Leconte, J., et al. 2014, A&A, 572, A109
Dieterich, S. B., Henry, T. J., Jao, W.-C., et al. 2014, AJ, 147, 94
Doyle, A. P. 2015, PhD thesis, Keele University
Fabrycky, D. & Tremaine, S. 2007, ApJ
Foreman-Mackey, D., Hogg, D. W., Lang, D., & Goodman, J. 2013, PASP, 125, 306
Gaia Collaboration, Brown, A. G. A., Vallenari, A., et al. 2016, A&A, 595, A2
Gill, S., Maxted, P. F. L., & Smalley, B. 2017, in prep
Gillon, M., Jehin, E., Delrez, L., et al. 2013, in Protostars and Planets VI Posters
Gillon, M., Jehin, E., Lederer, S. M., et al. 2016, Nature, 533, 221
Gillon, M., Jehin, E., Magain, P., et al. 2011, EPJ Web of Conferences, 11, 06002
Gillon, M., Triaud, A. H. M. J., Demory, B.-O., et al. 2017, Nature, 542, 456
Gillon, M., Triaud, A. H. M. J., Fortney, J. J., et al. 2012, A&A, 542, A4
Gray, R. O. & Corbally, C. J. 1994, AJ, 107, 742
Gustafsson, B., Edvardsson, B., Eriksson, K., et al. 2008, A&A, 486, 951
Gómez Maqueo Chew, Y., Morales, J. C., Faedi, F., et al. 2014, A&A
Henry, T. J., Jao, W.-C., Subasavage, J. P., et al. 2006, ApJ, 132
Hogg, D. W., Bovy, J., & Lang, D. 2010, ArXiv e-prints, arXiv:1008.4686v1
Jehin, E., Gillon, M., Queloz, D., et al. 2011, The Messenger, 145
Johnson, J. A., Apps, K., Gazak, J. Z., et al. 2011, ApJ, 730, 79
Kozai, Y. 1962, AJ, 67, 591
Kroupa, P. 2001, MNRAS, 322, 231
Lendl, M., Anderson, D. R., Collier-Cameron, A., et al. 2012, A&A, 544, A72
Lendl, M., Gillon, M., Queloz, D., et al. 2013, A&A, 552, A2
Lidov, M. L. 1961, Iskusst. Sputniki Zemli, 8, 5
Lopez-Morales, M. 2007, ApJ, 660, 732
Lucy, L. B. & Sweeney, M. A. 1971, AJ, 76, 544
Luger, R., Sestovic, M., Kruse, E., et al. 2017, Nature Astronomy, 1
Maxted, P. F. L. 2016, A&A 591, A111
Maxted, P. F. L., Serenelli, A. M., & Southworth, J. 2014, A&A 575
Pepe, F., Mayor, M., Rupprecht, G., et al. 2002, The Messenger, 110, 9
Petrovich, C. 2014, ApJ, 779
Pollacco, D. L., Skillen, I., Cameron, A. C., et al. 2006, PASP, 118, 1407
Queloz, D., Mayor, M., Udry, S., et al. 2001, The Messenger, 105, 1
Schwarz, G. 1978, The Annals of Statistics, 6, 461
Ségransan, D., Kervella, P., Forveille, T., & Queloz, D. 2003, A&A, 397, L5
Siverd, R. J., Beatty, T. G., Pepper, J., et al. 2012, ApJ
Southworth, J., Zucker, S., Maxted, P. F. L., & Smalley, B. 2004, MNRAS, 355, 986
Sullivan, P. W., Winn, J. N., Berta-Thompson, Z. K., et al. 2015, ApJ, 809, 77
Torres, G., Fischer, D. A., Sozzetti, A., et al. 2012, ApJ, 757, 161
Triaud, A. H. M. J., Hebb, L., Anderson, D. R., et al. 2013, A&A, 549, A18
Triaud, A. H. M. J., Neveu-VanMalle, M., Lendl, M., et al. 2017, MNRAS
Weiss, A. & Schlattl, H. 2007, Astrophysics and Space Science, 316, 99
Winn, J. N. 2010, ArXiv e-prints, arXiv:1001.2010v5
Winn, J. N., Holman, M. J., Torres, G., et al. 2008, ApJ, 683, 1076

## Appendix A: Radial-velocity data

Table A.1: CORALIE radial velocities of EBLM J0555-57A, and the probability that a point is not contaminated by the blend star. The radial velocity data are seperated into two sets, before and after $t_{JDB-2,400,000} = 56770.48$, to account for an upgrade of the instrument (Triaud et al. 2017). Separate systemic velocities are used for each set, determining $\gamma_1 = 19.537 \pm 0.015$ km s$^{-1}$, $\gamma_2 = 19.491 \pm 0.008$ km s$^{-1}$. All times are given in the $BJD_{UTC}$ timestamp.

| BJD - 2 400 000 day | RV km s$^{-1}$ | $1\sigma$ km s$^{-1}$ | FWHM km s$^{-1}$ | Bisector span km s$^{-1}$ | Depth of normalized CCF % | Probability | Spectrum rejected |
|---|---|---|---|---|---|---|---|
| 56610.686754 | 25.078 | 0.012 | 14.179 | 0.310 | 17.149 | 0.000 | x |
| 56615.797803 | 20.914 | 0.014 | 13.039 | 0.242 | 18.309 | 0.000 | x |
| 56629.624924 | 13.125 | 0.018 | 14.624 | 0.101 | 16.583 | 0.000 | x |
| 56640.778888 | 25.616 | 0.022 | 14.974 | 0.621 | 16.129 | 0.000 | x |
| 56641.641065 | 25.229 | 0.020 | 14.362 | 0.424 | 16.560 | 0.000 | x |
| 56644.700696 | 12.230 | 0.022 | 15.307 | 0.262 | 15.542 | 0.000 | x |
| 56695.539666 | 26.056 | 0.021 | 14.697 | 0.215 | 16.161 | 0.000 | x |
| 56697.572545 | 16.661 | 0.022 | 13.917 | -0.463 | 16.930 | N/A | x[a] |
| 56715.565737 | 15.302 | 0.014 | 13.869 | -0.056 | 17.264 | 0.560 | |
| 56716.588522 | 20.783 | 0.014 | 13.690 | 0.069 | 17.392 | 0.082 | |
| 56717.511413 | 24.949 | 0.023 | 13.837 | 0.071 | 16.637 | 0.873 | |
| 56718.547982 | 26.902 | 0.023 | 13.938 | 0.081 | 16.731 | 0.183 | |
| 56719.534391 | 24.542 | 0.023 | 13.828 | 0.215 | 16.913 | 0.962 | |
| 56723.625576 | 17.069 | 0.018 | 13.624 | -0.201 | 17.246 | 0.013 | |
| 56739.593653 | 19.399 | 0.015 | 13.797 | 0.012 | 16.991 | 0.726 | |
| 56740.590941 | 24.250 | 0.017 | 13.809 | 0.051 | 16.914 | 0.847 | |
| 56744.513089 | 13.487 | 0.020 | 13.866 | 0.073 | 16.544 | 0.610 | |
| 56746.538624 | 15.208 | 0.021 | 13.870 | -0.086 | 16.822 | 0.577 | |
| 56770.473218 | 19.968 | 0.021 | 9.1723 | 0.021 | 26.673 | N/A | x[b] |
| 56770.488252 | 18.650 | 0.020 | 13.668 | -0.045 | 17.040 | 0.059 | |
| 57082.579230 | 25.648 | 0.032 | 14.406 | 0.309 | 17.435 | 0.000 | x |
| 57085.612435 | 14.950 | 0.023 | 13.866 | -0.022 | 18.013 | 0.618 | |
| 57086.640474 | 11.384 | 0.022 | 14.154 | 0.338 | 17.643 | 0.000 | x |
| 57117.510586 | 11.564 | 0.032 | 14.182 | 0.158 | 17.501 | 0.000 | x |
| 57400.680862 | 26.035 | 0.030 | 14.424 | 0.260 | 17.408 | 0.000 | x |
| 57417.703102 | 24.652 | 0.025 | 13.768 | 0.079 | 18.222 | 0.527 | |
| 57420.648080 | 11.791 | 0.021 | 13.786 | 0.113 | 18.130 | 0.648 | |
| 57422.573335 | 21.016 | 0.026 | 13.674 | 0.067 | 18.352 | 0.090 | |
| 57772.591031 | 25.051 | 0.035 | 13.850 | 0.086 | 18.070 | 0.797 | |
| 57773.731230 | 26.807 | 0.025 | 13.916 | 0.000 | 17.930 | 0.296 | |
| 57774.695330 | 23.836 | 0.033 | 13.777 | 0.216 | 18.015 | 0.626 | |

**Notes.**
[a] Rejected before the FWHM outlier analysis due to anomalous span of the bisector inverse slope.
[b] Spectrum of EBLM J0555-57B